

# A Three-Dimensional Origami Paper-Based Device for Potentiometric Biosensing

Jiawang Ding<sup>+</sup>, Bowei Li<sup>+</sup>, Lingxin Chen, and Wei Qin\*

**Abstract:** Current paper-based potentiometric ion-sensing platforms are planar devices used for clinically relevant ions. These devices, however, have not been designed for the potentiometric biosensing of proteins or small molecule analytes. A three-dimensional origami paper-based device, in which a solid-contact ion-selective electrode is integrated with an all-solid-state reference electrode, is described for the first time. The device is made by impregnation of paper with appropriate bioreceptors and reporting reagents on different zones. By folding and unfolding the paper structures, versatile potentiometric bioassays can be performed. A USB-controlled miniaturized electrochemical detector can be used for simple and *in situ* measurements. Using butyrylcholinesterase as a model enzyme, the device has been successfully applied to the detection of enzyme activities and organophosphate pesticides involved in the enzymatic system as inhibitors. The proposed 3D origami paper device allows the potentiometric biosensing of proteins and small molecules in a simple, portable, and cost-effective way.

Potentiometry with ion-selective electrodes (ISEs) is a well-established technique that has been routinely used for the centralized analysis of a broad variety of ions and accounts for billions of measurements every year.<sup>[1]</sup> A potentiometric device usually consists of an ion-selective electrode, a reference electrode (RE) and an electrochemical detector. Solid-contact ISEs and REs with attractive features such as robustness, flexibility, cost-effective fabrication, and ease of miniaturization show exceptional promise for the construction of integrated devices.<sup>[2]</sup> The last few years have witnessed great advances in the design of solid-contact ISEs and REs and their applications for analytical devices.<sup>[3]</sup>

To reduce cost, simplify instrumentation, and incorporate functionality, paper has become a simple, flexible, and reliable platform for analytical devices.<sup>[4]</sup> Since the concept of microfluidic paper-based analytical devices ( $\mu$ PADs) was proposed by the Whitesides group, versatile  $\mu$ PADs have been developed with a variety of readout strategies, such as colorimetry, fluorescence, chemiluminescence, and amperometry.<sup>[5]</sup> Col-

orimetric and electrochemical methods are the preferred choices for  $\mu$ PADs. Compared with paper-based optical sensors, the electrochemical sensors are more quantitative and resistant to interference from color.<sup>[6]</sup> In recent years, potentiometric ISEs have been successfully integrated with  $\mu$ PADs. By exploring appropriate modifications of filter-paper substrates and making use of paper-based microfluidic sampling, planar platforms with various ISEs and REs have been proposed.<sup>[7]</sup> Unlike the disposable paper-strip ISE,<sup>[8]</sup> a whole potentiometric cell is embedded into the paper, which makes the device a truly useful diagnostic tool. Very recently, the Bühlmann group designed a promising condition- and calibration-free potentiometric ion sensing system,<sup>[9]</sup> which further simplifies the clinical applications. Although these methods have made great contributions to potentiometric ion sensing, the planar ion-sensing platforms developed so far are used only for clinically relevant ions such as sodium and potassium. No planar device has yet been designed for the potentiometric biosensing of proteins or small molecules.

$\mu$ PADs have evolved from two- to three-dimensional (3D) devices, and the development of 3D devices for rapid sensing is of special interest.<sup>[5e,10]</sup> 3D  $\mu$ PADs address the challenges of other paper-based analytical devices such as dipstick and lateral flow assays and can be used for multiplex assays. Flow control within 3D  $\mu$ PADs will broaden their applications in time-controlled signal amplification reactions, such as enzyme-linked immunosorbent assays.<sup>[11]</sup> Interestingly, the origami technique can be integrated with the fabrication of 3D  $\mu$ PADs, which provides a one-step method for patterning 3D paper devices.<sup>[10,12]</sup> In these 3D devices, the origami design can effectively eliminate problems of reagent diffusion by lateral flow in the channels of planar paper devices and thus avoid the incompatibilities of reagents (for example, enzymes and their substrates) located in different zones. Inspired by these advantages, we envisioned that 3D origami paper devices could be used to design potentiometric biosensing platforms for proteins and small molecule analytes. Such devices can be made by impregnation of paper with appropriate bioreceptors and reporting reagents at separate tabs. By folding and unfolding the paper structures, versatile potentiometric bioassays can be performed. To the best of our knowledge, a 3D origami paper device for potentiometric biosensing has not been reported.

Herein, we present a simple, robust, and practical 3D origami paper device by harnessing the merits of microfluidic paper-based assays and solid-contact-ISE-based potentiometry. A miniaturized detector (USB-controlled) that can perform simple and *in-field* testing was used for the electrochemical analysis. Butyrylcholinesterase (BuchE), which is

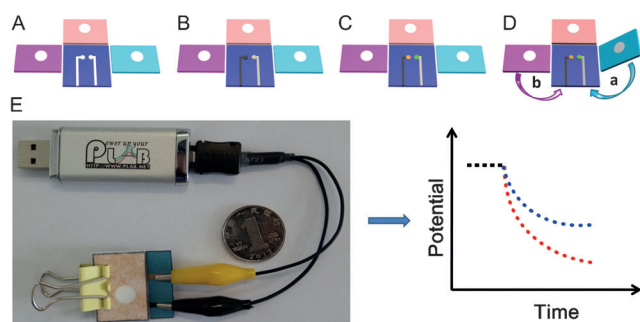
[\*] Dr. J. Ding,<sup>[+]</sup> Dr. B. Li,<sup>[+]</sup> Prof. L. Chen, Prof. W. Qin  
Key Laboratory of Coastal Environmental Processes and Ecological Remediation, Yantai Institute of Coastal Zone Research (YIC), Chinese Academy of Sciences (CAS); Shandong Provincial Key Laboratory of Coastal Environmental Processes, YIC-CAS  
Yantai, Shandong 264003 (P.R. China)  
E-mail: wqin@yic.ac.cn

[+] These authors contributed equally in this work.

Supporting information for this article can be found under:  
<http://dx.doi.org/10.1002/anie.201606268>.

a target enzyme for pesticide determination and drug screening and is also used as a label in immunoassays, was selected as a model. It is expected that the 3D origami paper device with the solid-contact ISE would be applicable for the rapid potentiometric detection of the enzyme and species involved in the enzymatic system.

The device was fabricated by using wax patterning to have a relatively high mechanical strength when wet, according to our previously described procedures (see the Supporting Information).<sup>[13]</sup> As shown in Scheme 1 A, the potentiometric



**Scheme 1.** Schematic of the 3D origami potentiometric paper-based device: A) without the carbon and Ag/AgCl electrodes; B) with the carbon and Ag/AgCl electrodes; C) with the ISE and RE membranes; and D) with the integrated cell for potentiometric detection. E) The origami paper-based device can be integrated with a miniaturized electrochemical analyzer (USB-controlled) for potentiometric biosensing.

$\mu$ PAD is comprised of one test pad surrounded by three folding tabs. On the test pad (bottom) layer, two linear regions of paper to be used as the substrates for the indicator and reference electrodes are separated by a 1.5 mm gap in the center position. In the folding tab layers, the whole paper is hydrophobic, owing to the printed wax, except for a round paper zone (i.d. 8 mm) in the center position to allow the sample or reagent solution to wick through and/or make contact with the ISE and RE membranes (for device dimensions, see Figure S1 in the Supporting Information). When sample or reagent solutions are added to the corresponding zones of the device, the geometry of the sensing zone allows ionic conductivity between the indicator electrode and the reference electrode. Additionally, sample handling and reagent immobilization functionalities can be integrated into the  $\mu$ PAD, which opens new opportunities for ISEs in potentiometric biosensing. For this design, one sheet of chromatography paper (A4, 210  $\times$  297 mm) can be used to fabricate 12 devices (Figure S2 in the Supporting Information).

In this work, carbon and Ag/AgCl inks were applied on the paper substrates by drop casting to prepare the carbon and Ag/AgCl electrodes, respectively (Scheme 1 B). Then, the ISE and RE membranes were formed by dip coating the cocktail solutions onto the carbon and Ag/AgCl supports, respectively (Scheme 1 C and the Supporting Information, Figure S3). It should be noted that carbon serves as not only the electrode substrate but also the ion-to-electron transducer. Indeed, it has been reported that carbon-based

materials can be used as transducers or components of PVC-based membranes for solid-contact ISEs.<sup>[3a,14]</sup> Contact angle measurements were carried out to confirm the properties of the carbon-ink-modified surface. The wax-printed paper and carbon-ink-printed surface show contact angles of  $150.4 \pm 1^\circ$  and  $143.1 \pm 2^\circ$  ( $n=3$ ), respectively. The carbon-ink-printed surface shows a high hydrophobicity, which could prevent the formation of a water layer between the polymeric membrane and the solid contact.<sup>[15]</sup> The bioassays on this 3D origami paper device can be performed manually through sequential and procedural folding of the tabs (Scheme 1 D). Moreover, this 3D origami system can be easily integrated and combined with a miniaturized electrochemical analyzer (Scheme 1 E) to develop a simple, sensitive, low-cost, and portable platform for point-of-care testing and on-site environmental monitoring.

Paper-based analytical devices that employ a printed Ag/AgCl reference electrode cannot maintain a stable potential unless a high and stable concentration of a soluble chloride salt is present in the sample solution.<sup>[16]</sup> Such requirement could limit the general applicability of the printed Ag/AgCl reference electrode. In this work, a solid-state reference electrode based on a poly(methyl methacrylate-co-butyl methacrylate) (MMA-BMA) membrane containing Ag/AgCl and KCl salt was constructed as described previously with some modifications (see the Supporting Information).<sup>[17]</sup> The commercially available copolymer MMA-BMA, which has a relatively slow salt leaching, was used as a matrix instead of polyacrylic polymers. Our preliminary experiments revealed that the reference electrode could show low potential variabilities to a wide range of chemical species (Figure S4 in the Supporting Information), redox pairs, and changes in pH, which is consistent with the results in the literature.<sup>[17a]</sup>

The performance of the newly developed paper-based devices was first evaluated for the use of ISEs for butyrylcholine. Our previous research has shown that a polymeric membrane electrode with high sensitivity and selectivity toward butyrylcholine can be designed by using heptakis(2,3,6-tri-*o*-methyl)- $\beta$ -cyclodextrin as an ionophore.<sup>[18]</sup> Since the choline cation generated by the butyrylcholine hydrolysis catalyzed by BuchE shows a much lower potential response than the butyrylcholine cation,<sup>[18b]</sup> the membrane ISE can be used for detection of BuchE activities. Herein, a solid-state butyrylcholine-sensitive membrane ISE was developed (see the Supporting Information). The thickness of the membrane was controlled by varying the volume of the cocktail solution deposited onto the sensing zone. The optimum volume of the cocktail solution for working and reference membranes with a relatively high stability was 10  $\mu$ L. To achieve a sensitive and rapid potentiometric biosensing, unconditioned membrane electrodes were used. Experiments revealed that a stable potential response could be obtained after circa 5 min (Figure S5 in the Supporting Information). Indeed, Lindner et al. reported that the equilibration times of solid-contact ISEs built on glass carbon and gold substrate could be short (ca. 5 to 10 min).<sup>[19]</sup>

The 3D origami device was operated by simply folding the three tabs along the fold-line following a specific sequence. In

this work, two layers on the device were required for the determination of enzyme activities (see the Supporting Information). The substrate tab was folded below the enzyme tab (Figure S6 in the Supporting Information). After folding, the device was clamped by binder clips to ensure contact. The measurements were done by using the reagent addition method. The substrate ions can wick to the enzyme zone, which initiates the enzymatic hydrolysis. The bioassay exhibits a linear response ( $r=0.99$ ) over the BuchE activity range from  $0.05$  to  $1.0 \text{ U mL}^{-1}$  with a detection limit of  $0.02 \text{ U mL}^{-1}$  ( $3\sigma$ ) (Figure 1). For the single-use device, device-to-device fabrication reproducibility was estimated by determining the potential response of  $0.5 \text{ U mL}^{-1}$  BuChE. The coefficient of variation was  $7.4\%$  ( $n=7$ ). It should be noted that the implemented BuchE sensing approach demonstrates a generic configuration applicable to many other enzymes and targets involved in enzymatic systems or enzyme-linked immunosorbent assays.

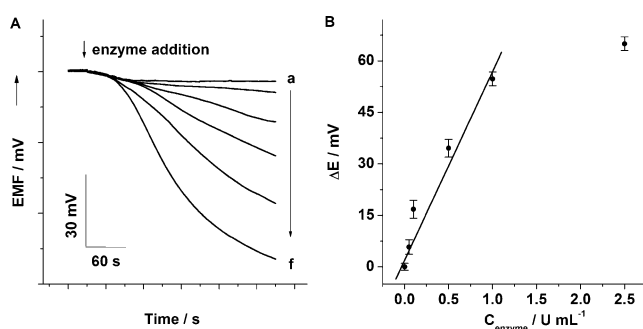


**Figure 1.** A) Potentiometric responses of the 3D origami paper-based device for  $10^{-3} \text{ M}$  substrate upon addition of BuchE at increasing concentrations: a) 0, b) 0.05, c) 0.1, d) 0.5, e) 1.0, and f)  $5.0 \text{ U mL}^{-1}$ . B) Calibration curve of the 3D origami potentiometric paper device for the determination of BuchE. Error bars represent standard deviation for three measurements.

Although only two layers on the device were required for the determination of enzyme activity, more complex analysis could be performed with the device. We next illustrate that the enzyme assays can be used to quantify small molecule analytes. It is well known that organophosphate pesticides (OPs) can irreversibly inhibit BuchE activity. A paper-based pesticide sensor for the determination of OPs based on BuchE inhibition was developed. As shown in Figure S7 in the Supporting Information, when  $0.5 \text{ U mL}^{-1}$  BuchE was added to the enzyme tab, the potential of the ISE decreased drastically (curve c), compared with the control (curve a). However, when  $0.5 \text{ U mL}^{-1}$  BuchE and  $1.0 \text{ nM}$  methyl parathion were added to the reagent tab at the same time, the potential change was smaller (curve b). This was because methyl parathion, as one of the OPs, can inhibit BuchE, thus reducing the enzymatic activity to its substrate. According to the well-established mechanism, the overall rate constant for the inhibition of the enzyme ( $k_i$ ) could be calculated (see the Supporting Information). An inhibition constant of  $k_i = 1.0 \times 10^5 \text{ M}^{-1} \text{ min}^{-1}$  could be obtained from the data shown in the Supporting Information, Figure S7 (Figure S8 in the Support-

ing Information). This value is in good agreement with the reported value.<sup>[20]</sup> To demonstrate the applicability of the device, the reagent-addition-based scheme was used for potentiometric determination of methyl parathion with high sensitivity (see the Supporting Information, Figure S9). Our experiments show that the proposed 3D  $\mu$ PADs enable the potentiometric biosensing of the pesticide, and the methodology can be useful for simple and in situ measurements.

To improve the portability, utility, and user-friendliness of the device, all the reagents involved in the sensing chemistry were included on the device in a dry state. We evaluated the potentiometric bioassays based on such user-friendly test format. In the present work, BuchE and substrate reagents were immobilized on different folding tabs by adsorption (see the Supporting Information). The morphologies of the paper and BuchE on the paper were characterized using scanning electron microscopy. As shown in the Supporting Information, Figure S10, the enzyme can adhere to the paper surface through physical trapping and van der Waals and electrostatic forces, which leads to a smoother surface. The BuChE activity on the paper was measured to be  $\text{ca. } 0.018 \pm 0.001 \text{ U}$  ( $n=3$ ) by using Ellman's method (Figure S11 in the Supporting Information).<sup>[21]</sup> In addition, bovine serum albumin was used as a stabilizer to prevent the thermally induced inactivation of enzyme.<sup>[22]</sup> Experiments showed that the enzyme activity could be maintained for a paper disk with adsorbed enzyme after storage at  $-20^\circ\text{C}$  for at least 12 days (Figure S12 in the Supporting Information).

The operation of the 3D origami-based device with immobilized reagents is shown in Figure 2A. The sample solution was added directly to the sample tab and then wicked to the enzyme-loaded tab. After incubation for 5 min at room temperature, the inhibited enzyme was placed in contact with the substrate tab to initiate the hydrolysis reaction (for more details on the folding sequence, see the Supporting Information). During measurements, the substrate ions diffused to the enzyme zones, where the enzymatic hydrolysis occurred. As shown in Figure 2B, a clear potential decrease can be observed in the absence of the pesticide, which indicates the preservation of the enzyme activity (Figure 2B). A distinct potential change can be observed when the sample contained the pesticide, and the potential change increased with increasing the methyl parathion concentration. In this proof-of-concept assay, the dynamic range is  $0.1\text{--}1.0 \text{ nM}$  methyl parathion and the limit of detection is  $0.06 \text{ nM}$  (Figure 2C). The detection limit is comparable to or even lower than those reported by other researchers.<sup>[23]</sup> The proposed devices not only are simple to operate but also have promising potential for the applications of ISEs by integration of binding, separation, and detection on a simple test-paper-like platform. Compared with strategies based on the lateral flow bioactive paper or dipstick sensing formats, the 3D  $\mu$ PADs would enable time-controlled incubation and enzymatic reactions.

In summary, we report for the first time a 3D origami paper device for potentiometric biosensing, which has the advantages of solid-contact ISEs for rapid sensing and of  $\mu$ PADs for simple operation and multiple functions. The paper-based device possesses several unique features. First,

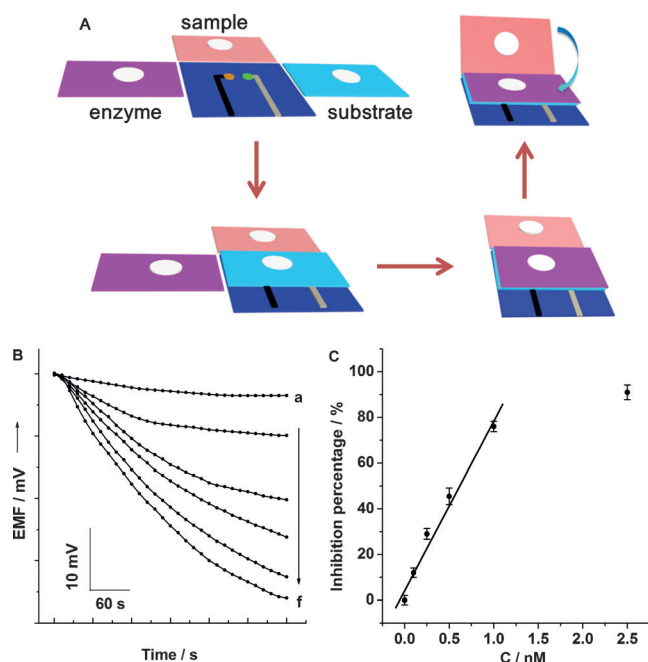


**Figure 2.** A) Schematic of the folding sequence for the potentiometric determination of methyl parathion. B) Potentiometric responses of the 3D origami device with immobilized reagents for a) 2.5, b) 1.0, c) 0.5, d) 0.25, e) 0.1, and f) 0 nM methyl parathion. C) Calibration curve of the 3D origami potentiometric device with immobilized reagents for detection of methyl parathion. Error bars represent standard deviation for three measurements.

compared with colorimetry, potentiometry is resistant to color or turbidity-induced interferences, which are usually encountered for real-sample bioanalyses. Second, the fabrication of the device is fast, easy, flexible, and inexpensive. Additionally, all fabrication steps could be easily automated. Third, the 3D structure makes it possible to control timing and has the potential for multiplex analyses. With other paper-based analytical devices such as dipstick and lateral flow assays, it is difficult to obtain multiplexed and quantitative results. Moreover, the application of this device to enzyme detection can promote the development of potentiometric immunoassays. Thus, we believe the proposed paper-based potentiometric device platform will be extensively used in the field of point-of-care testing and on-site environmental analysis.

## Acknowledgements

This work was financially supported by the National Natural Science Foundation of China (21575158, 21475148 and 21205131), the Strategic Priority Research Program of the Chinese Academy of Sciences (XDA11020702), the Youth Innovation Promotion Association of CAS (2013139), and the Taishan Scholar Program of Shandong Province.

**Keywords:** biosensors · enzyme-based assays · origami paper-based devices · potentiometry

**How to cite:** *Angew. Chem. Int. Ed.* **2016**, *55*, 13033–13037  
*Angew. Chem.* **2016**, *128*, 13227–13231

- [1] a) E. Bakker, P. Bühlmann, E. Pretsch, *Chem. Rev.* **1997**, *97*, 3083–3132; b) E. Bakker, E. Pretsch, *Angew. Chem. Int. Ed.* **2007**, *46*, 5660–5668; *Angew. Chem.* **2007**, *119*, 5758–5767; c) J. Bobacka, A. Ivaska, A. Lewenstam, *Chem. Rev.* **2008**, *108*, 329–351.
- [2] a) F. X. Rius-Ruiz, G. A. Crespo, D. Bejarano-Nosas, P. Blondeau, J. Riu, F. X. Rius, *Anal. Chem.* **2011**, *83*, 8810–8815; b) Y. Ishige, S. Klink, W. Schuhmann, *Angew. Chem. Int. Ed.* **2016**, *55*, 4831–4835; *Angew. Chem.* **2016**, *128*, 4912–4917.
- [3] a) T. J. Yin, W. Qin, *TrAC-Trends Anal. Chem.* **2013**, *51*, 79–86; b) J. B. Hu, A. Stein, P. Bühlmann, *TrAC-Trends Anal. Chem.* **2016**, *76*, 102–114; c) E. Bakker, *Anal. Chem.* **2016**, *88*, 395–413.
- [4] S. K. Mahadeva, K. Walus, B. Stoeber, *ACS Appl. Mater. Interfaces* **2015**, *7*, 8345–8362.
- [5] a) A. W. Martinez, S. T. Phillips, M. J. Butte, G. M. Whitesides, *Angew. Chem. Int. Ed.* **2007**, *46*, 1318–1320; *Angew. Chem.* **2007**, *119*, 1340–1342; b) R. V. Taudte, A. Beavis, L. Wilson-Wilde, C. Roux, P. Doble, L. Blanes, *Lab Chip* **2013**, *13*, 4164–4172; c) Y. Wang, L. Ge, P. Wang, M. Yan, S. Ge, N. Li, J. Yu, J. Huang, *Lab Chip* **2013**, *13*, 3945–3955; d) A. K. Yetisen, M. S. Akram, C. R. Lowe, *Lab Chip* **2013**, *13*, 2210–2251; e) D. M. Cate, J. A. Adkins, J. Mettakoonpitak, C. S. Henry, *Anal. Chem.* **2015**, *87*, 19–41; f) M. Cuartero, G. A. Crespo, E. Bakker, *Anal. Chem.* **2015**, *87*, 1981–1990; g) K. Yamada, T. G. Henares, K. Suzuki, D. Citterio, *Angew. Chem. Int. Ed.* **2015**, *54*, 5294–5310; *Angew. Chem.* **2015**, *127*, 5384–5401.
- [6] a) W. Dungchai, O. Chailapakul, C. S. Henry, *Anal. Chem.* **2009**, *81*, 5821–5826; b) E. J. Maxwell, A. D. Mazzeo, G. M. Whitesides, *MRS Bull.* **2013**, *38*, 309–314; c) J. Adkins, K. Boehle, C. Henry, *Electrophoresis* **2015**, *36*, 1811–1824; d) J. M. Oh, K. F. Chow, *Anal. Methods* **2015**, *7*, 7951–7960.
- [7] a) J. W. Cui, G. Lisak, S. Strzalkowska, J. Bobacka, *Analyst* **2014**, *139*, 2133–2136; b) M. Novell, T. Guinovart, P. Blondeau, F. X. Rius, F. J. Andrade, *Lab Chip* **2014**, *14*, 1308–1314; c) W. J. Lan, X. U. Zou, M. M. Hamed, J. B. Hu, C. Parolo, E. J. Maxwell, P. Bühlmann, G. M. Whitesides, *Anal. Chem.* **2014**, *86*, 9548–9553; d) J. B. Hu, K. T. Ho, X. U. Zou, W. H. Smyrl, A. Stein, P. Bühlmann, *Anal. Chem.* **2015**, *87*, 2981–2987.
- [8] a) M. Novell, M. Parrilla, G. A. Crespo, F. X. Rius, F. J. Andrade, *Anal. Chem.* **2012**, *84*, 4695–4702; b) S. T. Mensah, Y. Gonzalez, P. Calvo-Marzal, K. Y. Chumbimuni-Torres, *Anal. Chem.* **2014**, *86*, 7269–7273.
- [9] J. B. Hu, A. Stein, P. Bühlmann, *Angew. Chem. Int. Ed.* **2016**, *55*, 7544–7547; *Angew. Chem.* **2016**, *128*, 7670–7673.
- [10] a) H. Liu, R. M. Crooks, *J. Am. Chem. Soc.* **2011**, *133*, 17564–17566; b) H. Liu, Y. Xiang, Y. Lu, R. M. Crooks, *Angew. Chem. Int. Ed.* **2012**, *51*, 6925–6928; *Angew. Chem.* **2012**, *124*, 7031–7034; c) C. C. Wang, J. W. Hennek, A. Ainla, A. A. Kumar, W. J. Lan, J. Im, B. S. Smith, M. X. Zhao, G. M. Whitesides, *Anal. Chem.* **2016**, *88*, 6326–6333.
- [11] H. Noh, S. T. Phillips, *Anal. Chem.* **2010**, *82*, 4181–4187.
- [12] a) K. Scida, B. L. Li, A. D. Ellington, R. M. Crooks, *Anal. Chem.* **2013**, *85*, 9713–9720; b) L. Luo, X. Li, R. M. Crooks, *Anal. Chem.* **2014**, *86*, 12390–12397.
- [13] a) B. W. Li, W. Zhang, L. X. Chen, B. C. Lin, *Electrophoresis* **2013**, *34*, 2162–2168; b) B. W. Li, L. W. Fu, W. Zhang, W. W. Feng, L. X. Chen, *Electrophoresis* **2014**, *35*, 1152–1159.
- [14] a) C. Z. Lai, M. A. Fierke, A. Stein, P. Bühlmann, *Anal. Chem.* **2007**, *79*, 4621–4626; b) B. Paczosa-Bator, L. Cabaj, R. Piech, K. Skupień, *Anal. Chem.* **2013**, *85*, 10255–10261.
- [15] a) M. Fibbioli, K. Bandyopadhyay, S. G. Liu, L. Echegoyen, O. Enger, F. Diederich, P. Bühlmann, E. Pretsch, *Chem. Commun.* **2000**, 339–340; b) M. Fibbioli, W. E. Morf, M. Badertscher, N. F.

- de Rooij, E. Pretsch, *Electroanalysis* **2000**, *12*, 1286–1292; c) J. Sutter, A. Radu, S. Peper, E. Bakker, E. Pretsch, *Anal. Chim. Acta* **2004**, *523*, 53–59.
- [16] W. J. Lan, E. J. Maxwell, C. Parolo, D. K. Bwambok, A. Bala Subramaniam, G. M. Whitesides, *Lab Chip* **2013**, *13*, 4103–4108.
- [17] a) F. X. Rius-Ruiz, D. Bejarano-Nosas, P. Blondeau, J. Riu, F. X. Rius, *Anal. Chem.* **2011**, *83*, 5783–5788; b) F. X. Rius-Ruiz, A. Kisiel, A. Michalska, K. Maksymiuk, J. Riu, F. X. Rius, *Anal. Bioanal. Chem.* **2011**, *399*, 3613–3622.
- [18] a) J. W. Ding, W. Qin, *J. Am. Chem. Soc.* **2009**, *131*, 14640–14641; b) J. W. Ding, W. Qin, *Chem. Commun.* **2009**, 971–973.
- [19] M. Guzinski, J. M. Jarvis, B. D. Pendley, E. Lindner, *Anal. Chem.* **2015**, *87*, 6654–6659.
- [20] Y. C. Chiu, A. R. Main, W. C. Dauterman, *Biochem. Pharmacol.* **1969**, *18*, 2171–2177.
- [21] G. L. Ellman, *Arch. Biochem. Biophys.* **1959**, *82*, 70–77.
- [22] J. F. Tian, P. Jarujamrus, L. Z. Li, M. Li, W. Shen, *ACS Appl. Mater. Interfaces* **2012**, *4*, 6573–6578.
- [23] a) G. D. Liu, Y. H. Lin, *Anal. Chem.* **2005**, *77*, 5894–5901; b) X. C. Fu, J. Zhang, Y. Y. Tao, J. Wu, C. G. Xie, L. T. Kong, *Electrochim. Acta* **2015**, *153*, 12–18.

Received: June 28, 2016

Published online: September 16, 2016